INSTITUTE OF PHYSICS PUBLISHING NANOTECHNOLOGY
Nanotechnology **16** (2005) 1724–1733 doi:10.1088/0957-4484/16/9/053

Size-induced hysteresis in the process of nucleation and phase separation in a nanopowder

A S Shirinyan and M O Pasichnyy

Department of Physics, B. Khmelnytsky National University at Cherkasy, 81, Shevchenko Street, Cherkasy, 18031, Ukraine

E-mail: shirinyan@phys.cdu.edu.ua

Received 6 April 2005, in final form 14 June 2005
Published 6 July 2005
Online at stacks.iop.org/Nano/16/1724

Abstract
Peculiarities of kinetics of the solid–solid phase transition between single-phase and two-phase states in a nanopowder are considered here. We present a numerical assessment of the time-dependent behaviour of a supersaturated nanosystem undergoing temperature cycling. We demonstrate a distinct size-induced hysteresis and its peculiarities. The analysis indicates that as the system size decreases the hysteresis loop narrows, showing a tendency to disappearance. The model predictions are demonstrated for a sample system with general hypothetical properties. The results are found to depend on such thermodynamic and kinetic constraints as the size, the rate of temperature cycling, energy barriers for nucleation and diffusion, mechanisms of nucleation, and scatter in particle sizes of a nanopowder. The newly obtained results may be used for the achievement of an alternative method of information recording in present-day and future technologies.

1. Introduction

Due to their unique properties, first order phase transitions in nano-size systems play an important role in both scientific and technological fields [1, 2]. Despite their importance, understanding of these transitions is far from complete. So far there is no kinetic theory of separation, nor are there methods for controlling the formation of the bulk nanocrystalline materials, or forecasting of metastable phases in nanostates. In order to predict the properties of nanomaterials before their manufacturing, one must theoretically investigate these nanomaterials and the peculiarities of their behaviour in different situations, states and transformations.

It is known that a system which is quenched into the two-phase region separates via nucleation and growth of the new phase nuclei. Also, it is found that the boundaries of the first order phase transitions in nano-size systems deviate from the macroscopic ones due to the size effect [1, 3–5]. The structure of nanoparticles may change with the size, and also with the composition at constant size [6]. The explanation of size effects is generally related to additional energy of the external surface. Sometimes this property is interpreted in terms of additional energy under the curved surface due to Laplace tension [2, 7, 8]. Another effect arises for phase transitions in the multicomponent nanosize systems with change of composition, which was investigated by Rusanov in the 1960s. This is related to the limited number of atoms in a nanovolume, also known as the finite depletion effect [9–11]. So, when one extrapolates this argument to nanomaterials under various external conditions, one concludes that their kinetic behaviour should differ from that of the bulk material. There have been very few reports on the key role that size and finite depletion play in determining the properties and kinetic behaviour of the transforming nanosystem [12, 13].

Here we aim to elucidate the qualities of possible effects on the kinetics and the mechanism of phase transition in a nanopowder, rather than to obtain a realistic description of a specific binary system occurring in nature. While the theory presented here has a rather general character, one can report some specific applications of experimental interest for the theoretical approach developed in this paper. The origin of the presented results derives from the variation

0957-4484/05/091724+10$30.00

in energy with size and composition. So, one might expect the qualitative (and quantitative) conformance of the calculated with the experimental results in the case of the composition- and size-dependent material properties. In this respect, nanoparticles of Pb–Bi alloys have size-induced melting behaviour, observed by hot stage transmission electron microscopy [14]. The controllable, continuous and reversible phase coexistence of different crystalline and disordered phases in gallium nanoparticles under electron beam excitation has also been demonstrated [15]. It has been shown experimentally that the size dependence of structural solid–solid transition in CdSe semiconductor nanocrystals may indicate hysteresis behaviour [16, 17]. Moreover, recent theoretical, experimental and numerical Monte Carlo results on the first order phase transitions in nanovolumes demonstrate hysteresis phenomena [18–22].

We deal with a powder of nanosize particles subjected to temperature cycling, and present a numeric analysis within the framework of the standard kinetic equation approach. The present work is aimed at the study of the 'back-and-forth' transition during the temperature cycling and the evolution of such quantities as the mean composition in the parent phase and the volume fraction of the new phase. In other words, the objective of this paper is to describe the kinetics (unsteady-state kinetics of nucleation, new phase growth and separation) in the nanopowder related to

(i) the finite (non-negligible) depletion of the parent phase in nanoparticles of the powder;
(ii) finite rates of change of the external parameters (temperature changes during the annealing and heating);
(iii) the finite size of the system;
(iv) finite rates of the transfer of atoms across the parent phase–nucleus interface and bulk diffusion (existence of free energy barrier for diffusion);
(v) the effect of scatter in particle sizes (distribution of the nanoparticles);
(vi) mechanisms of nucleation (homogeneous or/and heterogeneous).

The structure of the paper is as follows.

In the next section we describe the thermodynamic model of phase transition. Here we present the analysis of the influence of size on thermodynamics when the final nucleation number, equilibrium size distribution, equilibrium mean composition in the parent phase and volume fraction of the new phase are obtained as functions of such thermodynamic parameters as the temperature and system size.

In section 3 we introduce the kinetic model of transition in the monodisperse nanopowder on the basis of a kinetic equation.

In section 4 we discuss and illustrate the unique features of the first order phase transitions—the hysteresis phenomenon based on the depletion and size effects. The corresponding modification for the case of scatter in particle sizes is presented in the appendix.

The concluding remarks are presented in section 5.

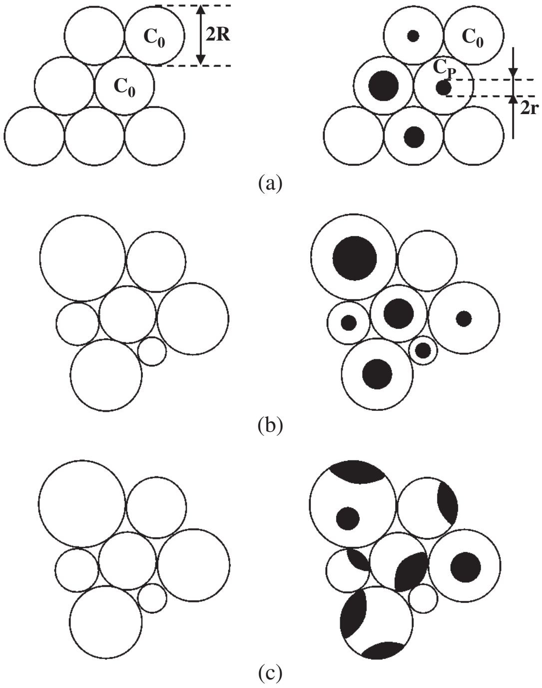

Figure 1. Nanopowder under the temperature cycling, i.e. particles of initial composition C_0 at high temperature and the same particles after the phase transition at low temperature: (a) case of equal size particles; (b), (c) case of scatter in particle sizes; (c) illustration of different mechanisms of nucleation. Each nanosized particle is described as isolated, each nucleus as a new phase inside the particle. C_p—concentration of the ambient parent phase after the nucleation.

2. Basic thermodynamic model

When dealing with nanoparticles, it is necessary to specify the size range under discussion and discuss the approximations, limits of applicability and specificities of nanosized particles. Indeed, in the literature, the term 'nanoparticle' is used for particles having sizes between a few atoms and clusters up to the 500 nm range. The behaviours of these nanoparticles are different. When the particles contain a few hundred atoms, the use of bulk parameters for describing nanosized binary particles may be not correct [22, and references therein]. Here, we treat cases where the thermodynamical description remains valid. This implies that the overall number of atoms in the particle is relatively large ($N_0 \geqslant 10^3$), where the classical nucleation theory is applicable.

2.1. *Transition modes*

Let us look at a binary system consisting of A and B components. Let us assume that small isolated initially supersaturated particles of a binary alloy are quenched into the two-phase region. Then a phase transition from the single-phase state to the two-phase one may occur in each particle (figure 1). As a first approximation, we arbitrarily assume that the new thermodynamically advantageous phase has strong stoichiometry $C_1 = 0.5$ (i.e. the atomic concentration). The composition in each initially supersaturated solid particle is equal to C_0 (so that the new phase nucleus has a composition different from the parent phase one, $C_1 \neq C_0$). Hereinafter, the starting phase is also called the 'parent' or 'old' phase and the newborn phase is called phase 1 and will have subindex 1.

At first we restrict the discussion to the thermodynamics of a single particle.

2.2. *Driving force*

Now let us consider the driving force of the phase transition. It is necessary to consider the free energy of the new phase, relative to that of the parent phase. Since the considered temperatures are well above the Debye temperature, the specific heat is approximately constant. Hence, for the formation of a two-phase system, where the new phase has a non-zero driving force of transformation, one can write

$$\Delta g_0(T, C) = kT(C\ln(C) + (1-C)\ln(1-C)). \qquad (1)$$

$$\Delta g_1(T) = \Delta g_1 + \alpha kT, \qquad (C = C_1). \qquad (2)$$

Here α, Δg_1 are parameters of the system, k is the Boltzmann constant, T the absolute temperature, $\Delta g_0(T, C)$ is the Gibbs free energy (per atom) of the parent supersaturated phase and $\Delta g_1(T)$ is the Gibbs free energy of formation of the new phase 1.

2.3. *Depletion*

Usually, when nucleation is considered, it is assumed that the reservoir of matter is very large. In nanosystems, it is quite the opposite. If a nanosystem is quenched into the two-phase region, then, in addition to the size effect, the depletion of the surrounding parent phase may occur because of the difference in C_0 and C_1 compositions. Hence one must also take into account the fact that not all stoichiometries are available, due to the above-mentioned finite quantity of matter [21]. The mole fractions C_1 and C_p of species B in the new and parent phases, respectively, are interrelated by the conservation law:

$$C_0 N_0 = C_1 N_1 + C_p N_p, \qquad (3)$$

where N_1 is the number of atoms in the newly formed cluster of the new phase (2) and N_0 and N_p ($N_p = N_0 - N_1$) are the numbers of atoms in the parent phase before transition and after nucleation, respectively.

2.4. *Energy of transition*

The change in Gibbs free energy (per particle) in the case of nucleation may be expressed as

$$\Delta G(N, T) = \Delta g_1(T)\frac{N}{C_1} + \Delta g_0(T, C_p(N)) \times \left(N_0 - \frac{N}{C_1}\right) - \Delta g_0(T, C_0)N_0 + K\left(\frac{N}{C_1}\right)^{2/3}, \qquad (4)$$

where N is the number of structural units AB in the new stoichiometric phase (interrelated with the number of atoms N_1 in the same phase: $N = C_1 N_1$), $K = 3(4\pi/3)^{1/3}\sigma n^{-2/3}$ is the coefficient of the surface energy contribution and σ is the specific interphase energy on the parent phase–nucleus interface. Hereinafter the number of atoms per unit volume n is presumed to be the same for the old and new phases ($n_1 = n$).

2.5. *Equilibrium distribution*

The previous discussion deals with values of the thermodynamic parameters, as applied to a single nanoparticle. Under experimental conditions, one generally deals with a large number of particles. It is therefore mandatory to study the phase transition of nanoparticles using a statistical approach by considering the size distribution function.

Under equilibrium, the probability of the first order phase transition is given by the theory of thermodynamic fluctuations. The equilibrium in a nanopowder will correspond to the statistic distribution, in which, at any moment of time, at the given T, some of the particles will be in single-phase states and the rest in two-phase states (figure 1(a)). The corresponding number of particles, $f_{eq}(N, T)$, in which the new phase nucleus consists of N structural units AB, may be found by the Boltzmann formalism:

$$f_{eq}(N, T) = \frac{W}{\sum_{N=N_{min}}^{N_{max}} \exp\{-\frac{\Delta G(N,T)}{kT}\}} \exp\left\{-\frac{\Delta G(N, T)}{kT}\right\}. \qquad (5)$$

Here W is the total number of nanoparticles in the powder. N_{min} is the minimum number of structural units in the new phase nuclei. According to the conservation of matter (3), at every fixed T, there exists the constraint on the maximum number of atoms in the nucleus of the new phase 1. This number cannot be bigger than $N_0 C_0/C_1$ (when the parent phase is fully depleted by B-species, $C_p = 0$). So the maximum number of structural units in each nucleus should not be bigger than $N_{max} = N_0 C_0$. Hereby the change of Gibbs free energy (4) at this limit point N_{max} has the tendency to increase rapidly [9–11].

2.6. *Varying T and N_0*

Let us first examine the consequences of the temperature changes on the variation of thermodynamic quantities $\Delta G(N, T)$ and $f_{eq}(N, T)$ with other parameters fixed [22].

At a high T, the $\Delta G(N, T)$ dependence on N is increasing (and the dependence of $f_{eq}(N, T)$ on N is decreasing). This is the case of the prohibition of the phase transition. When T decreases, the dependences of $\Delta G(N, T)$ and $f_{eq}(N, T)$ on N change from monotonic curves to nonmonotonic ones with one maximum and one minimum. A simple analysis of equations (4) and (5) shows that the minimum of the $f_{eq}(N, T)$ curve corresponds to the maximum of the $\Delta G(N, T)$ curve and vice versa. Also, the nonzero maximum of $f_{eq}(N, T)$ (and the nonzero minimum of $\Delta G(N, T)$) corresponds to the two-phase equilibrium state of the nanopowder (figure 1). Hereby, the lower T, the bigger are the average sizes of the supercritical nuclei of the new phase at equilibrium conditions.

Similar conclusions are true with respect to the varying of N_0 with other parameters fixed [13, 22, 23]. As is shown, when N_0 is rather small, the nucleation is impossible. Thus, the limited volume of the nanopowder particles constrains the composition fluctuations, as well as the fluctuations of the new phase, and allows one to keep the alloy nanopowder in a state which would have been unstable in the case of a bulk.

2.7. *Mean composition in depleted parent phase at equilibrium*

Let us recall here that the present work intends to investigate the evolution of the mean composition in the depleted parent phase and of the volume fraction of the new phase (shown below). The corresponding equilibrium mean composition $\langle C_{\mathrm{p}}^{\mathrm{eq}} \rangle$ in the parent phase and the equilibrium volume fraction of the new phase ρ_{eq} are found by ratios:

$$\langle C_{\mathrm{p}}^{\mathrm{eq}} \rangle = \frac{\sum_{N=N_{\min}}^{N_{\max}} C_{\mathrm{p}}(N) f_{\mathrm{eq}}(N,T)(N_0 - \frac{N}{C_1})}{\sum_{N=N_{\min}}^{N_{\max}} f_{\mathrm{eq}}(N,T)(N_0 - \frac{N}{C_1})},$$
$$\rho_{\mathrm{eq}} = \frac{\sum_{N=N_{\min}}^{N_{\max}} \frac{N}{C_1} f_{\mathrm{eq}}(N,T)}{N_0 W}. \tag{6}$$

Found by such a procedure, the equilibrium mean composition in the parent phase and the volume fraction of the new phase are obtained as functions of T and N_0.

3. Basic kinetic model

3.1. *Temperature cycling*

Let us now introduce the finite rates of temperature change and consider the temperature cycling. First, we start from the single-phase state at high T (figure 1) and let T decrease (cooling). Then we stop the temperature at some point, when the alloy is quenched into the two-phase region, and reverse the direction, i.e. increase T (heating) at the same rate. One cycle refers to the complete to-and-fro changes of T from some initial point back to the same point, say from $T = 1100$ K to $T = 800$ K back to $T = 1100$ K. The corresponding 'decoding' of 'back-and-forth' transformation is made within the framework of the kinetic equation approach. In the case considered here, the temperature T will change in time as a linear function with constant rate $|\mathrm{d}T/\mathrm{d}t| =$ constant for cooling and heating. The Gibbs free energy (4) may be expressed as the function of time (via the time-dependent temperature): $\Delta G(N,T) \equiv \Delta G(N,t)$.

3.2. *Evolution of distribution function*

Let us consider the non-equilibrium size distribution function $f(N,t)$—the number of new phase droplets consisting of N structural units at the moment of time t. As mentioned above, $C_0 < C_1$, $C_1 = 0.5$, so the process is controlled by B component mobility. The evolution of the ensemble of clusters formed by nucleation and growth processes will be described by the kinetic equation

$$\frac{\partial f(N,t)}{\partial t} = f(N-1,t)\upsilon_+(N-1) + f(N+1,t) \times \upsilon_-(N+1) - f(N,t)(\upsilon_-(N) + \upsilon_+(N)). \tag{7}$$

The frequencies of attachment $\upsilon_+(N) \equiv \upsilon_+(N,T)$ and detachment $\upsilon_-(N) \equiv \upsilon_-(N,T)$ of monomers AB to a cluster of size N are interrelated as [24]

$$\upsilon_-(N,T) = \upsilon_+(N,T)\exp\left(\frac{\Delta G(N,T) - \Delta G(N-1,T)}{kT}\right). \tag{8}$$

One usually distinguishes two kinds of kinetic redistribution of components: for a so-called diffusion-control (bulk) process and for a kinetic-control (surface) process.

For nanometric particles, interdiffusion of atoms can be much faster than in bulk binary materials, by several orders of magnitude [25]. This means that the diffusion barriers may be significantly lower than in the bulk. Moreover, in the case of nanosized particles the surface diffusion has to be the key role. This is more and more likely as the size decreases. That is why, in the following, the quantity $\upsilon_+(N,T)$ will be taken as that of the kinetic-control process [24]: $\upsilon_+(N,T) = MDC_{\mathrm{p}}N^{2/3}$. Hereby, M is the constant of the material, and the temperature-dependent coefficient of diffusion D of ambient phase B-species located in the vicinity of the nucleus of the new phase will obey the Arrhenius law: $D = D_0\exp(-Q/kT)$ with the activation energy Q of diffusion. The quantitative expression for the frequency $\upsilon_+(N,T)$ is obtained by considering the growth of the new phase clusters that have to result from a series of monomolecular additions to the nucleus. In the case of solid-to-solid phase transition, this process will require a diffusional hop across the interface and activation energy Q for the jump across the interface. The quantity Q may be presumed to be similar to that required for diffusion in the solid parent phase: $Q \approx 18kT_m$ (T_m—the temperature of melting). So, in our following consideration we use a new nondimensional variable for the time $\tau = MD_0t$ and the corresponding rate $\upsilon = |\mathrm{d}T/\mathrm{d}\tau|$.

Let us first consider the case of equal size particles (modification is presented in the next section). In this case the cluster size distribution function $f(N,\tau)$ obeys boundary conditions (which are reduced to the conservation of particles):

$$f(N_{\min},\tau) = W - \sum_{N_B=N_{\min}+1}^{N_{\max}} f(N,\tau),$$
$$f(N_{\max},\tau) = 0, \tag{9}$$
$$f(N,\tau=0) = \begin{cases} W, & N = N_{\min} \\ 0, & N \neq N_{\min}. \end{cases}$$

3.3. *Evolution of average composition and volume fraction*

Further, we want to show the evolution of the average composition $\langle C_{\mathrm{p}} \rangle$ of the depleted parent phase and the volume fraction ρ of the new phase. The corresponding values are determined by formulae:

$$\langle C_{\mathrm{p}} \rangle = \frac{\sum_{N=N_{\min}}^{N_{\max}} C_{\mathrm{p}}(N) f(N,\tau)(N_0 - \frac{N}{C_1})}{\sum_{N=N_{\min}}^{N_{\max}} f(N,\tau)(N_0 - \frac{N}{C_1})},$$
$$\rho = \frac{\sum_{N=N_{\min}}^{N_{\max}} \frac{N}{C_1} f(N,\tau)}{N_0 W}. \tag{10}$$

3.4. *Algorithm of numeric calculations*

We introduce the number of particles W and their sizes N_0, then trace the driving force of transformation $\Delta G(N,T)$ for every particle at each evolution stage, then count the number of separated particles $f(N,\tau)$ in the nanopowder, $\langle C_{\mathrm{p}} \rangle$ and ρ during the temperature cycling.

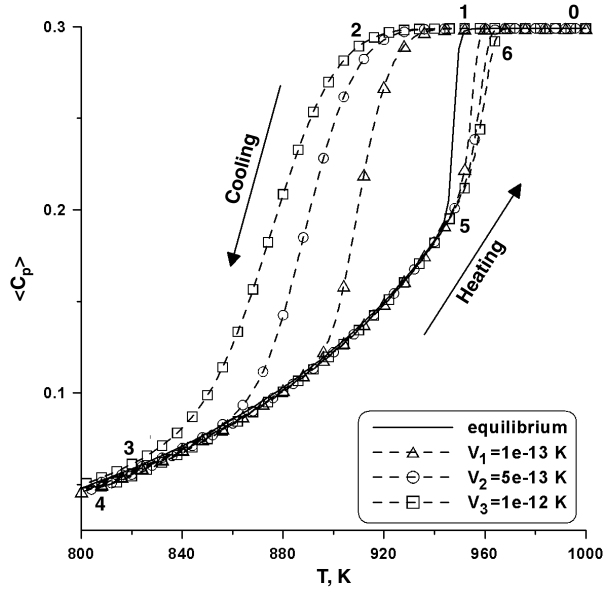

Figure 2. Representation of the hysteresis effect in the powder of nanosize particles related to the finite size and depletion: mean composition $\langle C_\mathrm{p}\rangle$ in depleted parent phase versus temperature T (for three different constant rates $\upsilon_1 < \upsilon_2 < \upsilon_3$, $\upsilon_1 = 10^{-13}$ K; $\upsilon_2 = 5\times10^{-13}$ K, $\upsilon_3 = 10^{-12}$ K). Parameters are presented in the main text. The solid line characterizes equilibrium values $\langle C_\mathrm{p}^\mathrm{eq}\rangle$.

4. Hysteresis—results and discussion

When the rate of T change is finite, one can observe hysteresis behaviour, as shown below. Let us choose as the numerical values of parameters of the binary nanosystem the typical values for intermetallic systems. Numeric calculations in this paragraph have been realized for the following set of parameters: $C_0 = 0.3$, $C_1 = 0.5$, $N_\mathrm{min} = 2$, $W = 10^{10}$, $\Delta g_1 = -4.5\times10^{-20}$ J, $\alpha = 2.3$, $\upsilon = 5\times10^{-13}$ K, $Q = 18\,kT_m$, $T_m = 1200$ K, $N_0 = 1000$, $K = 3\times10^{-20}$ J. The temperature will change in time from 1100 to 800 K and back to 1100 K with different constant rates $\upsilon = |\mathrm{d}T/\mathrm{d}\tau|$: $\upsilon_1 = 10^{-13}$ K, $\upsilon_2 = 5\times10^{-13}$ K, $\upsilon_3 = 10^{-12}$ K, $\upsilon_4 = 5\times10^{-12}$ K, $\upsilon_5 = 5\times10^{-11}$ K and $\upsilon_6 = 1\times10^{-10}$ K. Values N_0, T, υ, Q and K will also be pointed out in each simulation experiment separately, if they differ from the mentioned ones.

In this section we report the newly obtained result: size-induced hysteresis. Our model shows that the width and shapes of hysteresis loops depend on N_0, $\mathrm{d}T/\mathrm{d}\tau$, σ or K, Q and scatter in particle sizes. The separation kinetics related to the different rates of temperature change is now investigated. Hereby we shall alternately show $\langle C_\mathrm{p}\rangle$ and ρ.

4.1. Varying $dT/d\tau$

The process of temperature cycling from high T to low T and back, with other parameters fixed, is shown in figure 2. Please note that the evolution of $f(N,\tau)$ becomes a very slow process at low T because of the temperature-dependent diffusion coefficient D.

Let us briefly discuss, for example, the case of υ_3 in figure 2. The temperature cycling leads to the $\langle C_\mathrm{p}\rangle$ curve—the evolution path 01234560. Hereby, one distinguishes

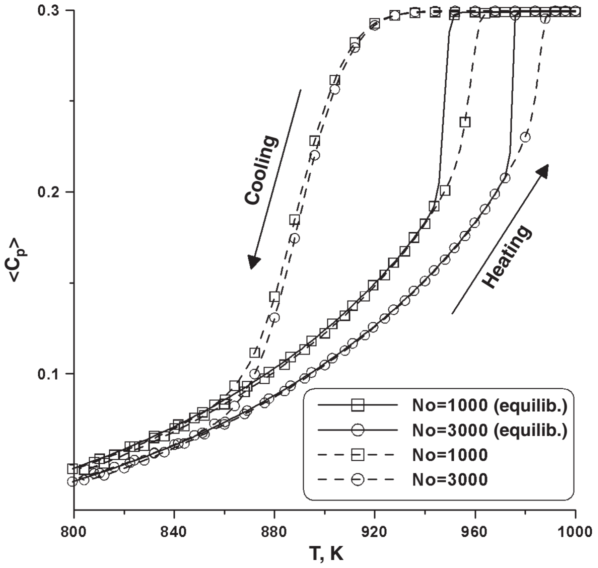

Figure 3. The influence of sizes N_0 on hysteresis loops (for the same rate $\upsilon = \upsilon_2$ and the different N_0: $N_0 = 1000$, $N_0 = 3000$). Solid lines characterize the equilibrium values $\langle C_\mathrm{p}^\mathrm{eq}\rangle$ at N_0 =1000 and $N_0 = 3000$, respectively.

012—supersaturated single-phase state (parent phase) of the nanopowder (see also figure 1),

23—phase transition from the single-phase state at point 2 to a two-phase state (parent phase + new phase 1) at point 3 (this event indicates the nucleation),

34, 45—cooled and/or superheated two-phase states (parent phase + new phase 1)—and

56—back transition from the (parent phase + new phase 1) state at point 5 to the parent phase state at point 6.

The slope of branch 23 depends on cooling conditions (as well as the slope of curve 56 depending on heating conditions). The solid line characterizes the coinciding 'back-and-forth' evolution of equilibrium values $\langle C_\mathrm{p}^\mathrm{eq}\rangle$ found by equation (6).

It is worth noting that the shown hysteresis is very similar to magnetic (such as paramagnetic–ferromagnetic) phase transitions under the applied magnetic field. Such behaviour should allow for the usage of the size-induced hysteresis effect in a way similar to that of magnetic materials for a variety of applications.

As one can see, the width of hysteresis loops (the effective length between left and right branches of curve $\langle C_\mathrm{p}\rangle$ in intermediate temperature intervals) depends on the rate of temperature change. Namely, the greater the rate υ, the bigger the effective width of hysteresis loops. As the value υ decreases, the hysteresis loop narrows. In fact, the hysteresis clearly shows that the evolution of the size distribution function $f(N,\tau)$ does not coincide with the evolution of the equilibrium distribution function $f_\mathrm{eq}(N,\tau)$. As soon as the temperature is stopped the system relaxes and $f(N,\tau)$ tends to $f_\mathrm{eq}(N,\tau)$, while ρ tends to ρ_eq and $\langle C_\mathrm{p}\rangle$ to $\langle C_\mathrm{p}^\mathrm{eq}\rangle$.

4.2. Varying N_0

Now, let us examine the influence of different values of N_0 (effect of different sizes). The corresponding result, at fixed rate υ_2 and for other parameters fixed, is presented in figure 3.

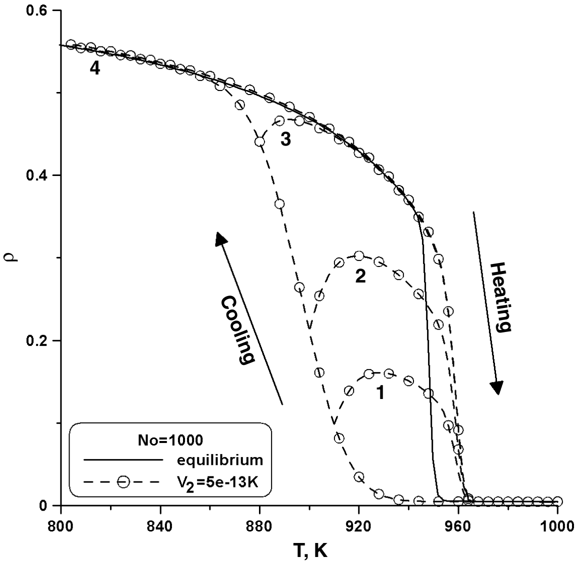

Figure 4. The evolution of volume fraction ρ during the process of to-and-fro changes of temperature T and different low boundaries of temperature: 1—for low limit $T_{\min 1} = 910$ K, 2—for $T_{\min 2} = 900$ K, 3—for $T_{\min 3} = 880$ K, 4—for $T_{\min 4} = 800$ K.

We see that the bigger the system size is, the greater is the effective width of the hysteresis loop under the same cycling conditions. (The smaller the size of the particles is, the smaller is the effective width of the hysteresis loop.)

It is the first time, as far as we know, that a distinct conclusion about the tendency of hysteresis to narrow and disappear with the decrease of the size of a system has been obtained.

In figure 3, the left branches of hysteresis loops for different N_0 almost coincide, whereas the right branches differ considerably. Nevertheless, simulations show that for smaller υ the difference of left branches of loops also increases. (The reason is that the system becomes closer to the corresponding equilibrium; consequently, the $\langle C_\mathrm{p}\rangle$ curve becomes closer to the $\langle C_\mathrm{p}^\mathrm{eq}\rangle$ curve.)

4.3. *Influence of temperature boundaries of cycling*

Consider now the evolution of ρ and $\langle C_\mathrm{p}\rangle$ in the case of different low boundaries of temperature cycling. Let us recall here that, first, we decrease T starting from high values, then stop and increase T at the same rate until the starting point is reached. Choosing different low limiting values of temperature cycling, one should investigate their influence on the hysteresis loop's shape. The result is shown in figure 4 (for the case $\upsilon = \upsilon_2$).

One can see the inertia effect of the system represented by figure 4. There exist some temperature intervals in which the ρ curve increases (and the $\langle C_\mathrm{p}\rangle$ curve decreases) even after the turn-point temperature. This is the effect of nonsteady kinetics. Such intervals show separation—the transition from the single-phase state to the two-phase state (figure 1). It means that in this case the increasing of T (after the turn-point) leads to an inverse (abnormal) process, whereas usually it must be the collapsing of the nuclei and transformation of two-phase particles into single-phase particles. In other words, when the direction of temperature variation is changed, there exist some time intervals where most of all overcritical nuclei grow, whereas the driving force decreases.

The appearance of the hysteresis loops presented here is related to the thermodynamic constraints, namely, the nucleation barrier existence, nonmonotonic and asymmetric $\Delta G(N, T)$ dependence on N at any moment of time. The $\Delta G(N, T)$ shape leads to different fluctuation time values between the forth transition (nucleation and separation), and the back transition (from the two-phase state to the single-phase state).

In general, both thermodynamic as well as kinetic factors result in the existence of hysteresis. This is obvious from the results obtained in the present work, in particular from the fact that the changing of Q, υ or K always changes the hysteresis loop, its width and the shape. Hereby one needs to differentiate two cases: cases of slow rates υ (when the rate of change of the external parameters is slower than the rate of nucleation-growth processes) and cases of high rates υ.

4.4. *Varying Q and K at slow υ*

To see the influence of kinetic constraints we should establish different values of activation energy Q for the diffusion jump across the interphase. In this study we have used three different activation energies $Q_1 = 18\ kT_m$, $Q_2 = 16\ kT_m$ and $Q_3 = 15\ kT_m$ and found that the smaller Q is (that is, the bigger D is), the less is the effective width of hysteresis.

Similar reasoning is applied to the influence of σ or K. As the value of interphase tension decreases, the hysteresis loop narrows (for fixed rate υ_2 and other parameters). In particular, in the limit case $\sigma = 0$ and slow rate $\upsilon = \upsilon_2$ (and nonzero Q, fixed cycling conditions and other mentioned parameters) the hysteresis disappears.

In order to separate the kinetic from the thermodynamic size effects on the phase transition one should discuss the case of $\sigma = 0$ for different high rates υ.

4.5. *Varying υ at zero nucleation barrier height* ($K = 0$)

In the limit case when $K = 0$, the nucleation barrier becomes zero. In this case, at high υ, the existence of hysteresis may take place mainly due to the kinetic factor Q. The corresponding comparison is shown in figure 5.

At first, for high T, the diffusion coefficient D is big, so that the evolution of the $f(N, \tau)$ function is also fast and coincides with the $f_\mathrm{eq}(N, \tau)$ distribution evolution. As the T decreases, the value D decreases, too. In other words, at low T, the hysteresis curve becomes essentially different from the equilibrium one ('aubergine' or 'pelican' shape of hysteresis loop)—freezing effect. Besides this, one can see that the width of hysteresis is different for high T, low T and intermediate values. At intermediate intervals of T the width (length between the braches) of the hysteresis is smaller. Let us recall here that at high T, due to depletion, $\Delta G(N, T)$ is a monotonic increasing function, whereas at low T, $\Delta G(N, T)$ has no nucleation barrier. Thus, one comes to a conclusion that at high T the hysteresis is conditioned mainly by a thermodynamic controlled process, whereas at low T the hysteresis is conditioned by a kinetic controlled process.

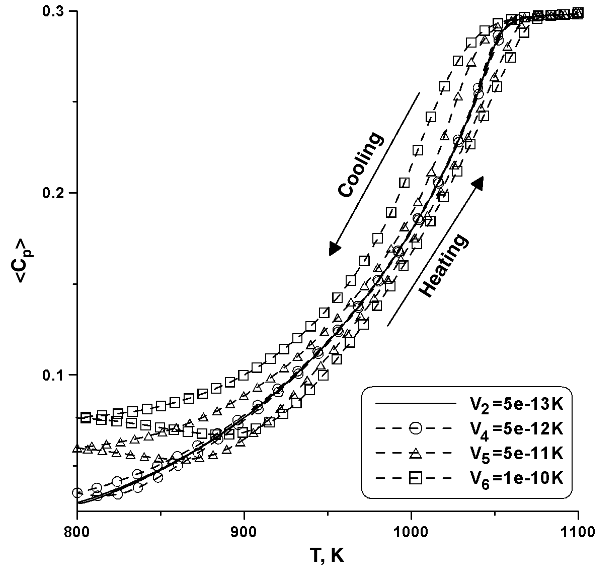

Figure 5. 'Pelican'-like hysteresis loops. The demonstration of the dominant influence of kinetic constraints on hysteresis at low T—effect of freezing. The lengths between the branches of hysteresis are different for low T, high T and intermediate T. The result is presented for different rates υ at $K = 0$ ($\sigma = 0$), $N_0 = 1000$ and other mentioned parameters.

One may expect that the 'pure' hysteresis loop presented here will be different from the real experimental one [17, 18]. This is caused by the existence of irregularities, defects of any kind, particle size distribution, and diffusion between the particles of a powder in real experiments, which will lead to a shift of the separation and/or nucleation points, barriers etc.

4.6. *Effect of scatter in particle sizes*

The previous reasoning is based on the assumption that the nanopowder consists of equal size particles. In real experiments, this is far from true. Even if one wants to prepare monodisperse nanopowder, still a distribution in particle sizes exists. Experimental studies usually show that the highly monodisperse particles in a powder have a standard deviation of less than 5–10% [16, 19, 26]. So, one has to calculate cases where the size distribution of nanoparticles takes place (figure 1(b)). It is obvious that equations (3)–(10) must be reformulated. The corresponding approach is used in the appendix.

In fact, the existence of scatter in particle sizes may lead either to the broadening of the hysteresis loop or to its narrowing. The result depends on the type of size distribution: either symmetric or not, with respect to the most probable size $\bar{N}_0$ (figure 1(b)). For small deviations, the value $\bar{N}_0$ is almost coincident with the mean size N_0.

Here we formulate our analysis for two kinds of distributions usually obtained under experimental conditions: a symmetric Gaussian distribution and an asymmetric lognormal distribution [26]. In the following, we consider the system at the above-mentioned parameters and different deviations δ. The result of investigation of the influence of scattering in particles sizes is shown in figure 6.

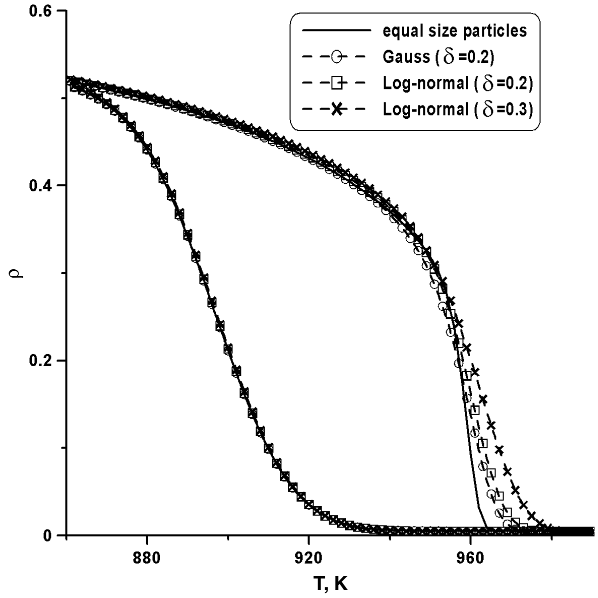

Figure 6. Effect of scatter in particle sizes on the hysteresis loops for Gaussian and lognormal distributions with different deviations δ (see the appendix). Parameters are presented in the main text.

We see that small deviations ($\delta < 0.2$) practically do not change the shape of the hysteresis whereas the width appears slightly increased at high T. In the case of lognormal distribution the increase of δ leads to an increase in the hysteresis loop due to the shape of the distribution (figure A.1(b)). In other words, there are a small number of very small particles and a big number of very large particles present.

Influence of different nucleation mechanisms. The objective of this section is to relate the value of a parameter describing the nucleation mechanism to the shape of the hysteresis loop. We chose the lognormal form for further investigation, as these distributions are commonly seen in experimental systems. The mechanism of nucleation has an influence on the nucleation barrier height. (This contribution is partially discussed in paragraph 4.5 for the case of equal size particles.) Let us ignore the assumption that inside a nanoparticle only one nucleus is formed (figure 1(c)). In the simple form, the corresponding simulation experiments may be carried out by varying the coefficient K. For this purpose, we divide the powder into 20 groups of different sizes (shown below) and different values of K, where K can be only of two kinds ($K_1 = K = 3 \times 10^{-20}$ J, $K_2 = K/2$), and investigate the transformation as a function of T and K with other parameters and cycling conditions fixed. Such a procedure is based on the assumptions that (i) inside the particle not only one cluster can be formed, (ii) there exist different nucleation mechanisms (say, homogeneous, at $K = K_1$, inside the particles and heterogeneous on the external surface of particles, at $K = K_2$). This may be of tremendous importance, if the size of the particles increases.

Actually, we divided each of the ten previously mentioned (see the appendix) groups W_i ($i = \overline{1, 10}$) into two subgroups W_{i1} and W_{i2} proportionally to W_i ($W_{i1}+W_{i2} = W_i$, $W_{i1} = \beta W_i$ and $W_{i2} = \{1 - \beta\}W_i$). In each subgroup the value of

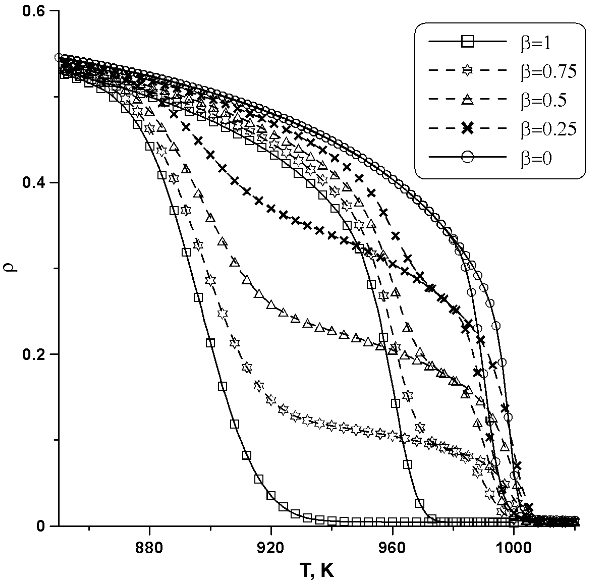

Figure 7. Influence of different mechanisms of nucleation on hysteresis loops for lognormal distribution ($\delta = 0.2$, table A.2 of the appendix). $K_1 = K = 3 \times 10^{-20}$ J, $K_2 = K/2$. Explanation is given in the text.

coefficient K is taken as K_1 or K_2, respectively. Under the chosen conditions, the coefficient β indicates what part of the particles undergoes homogeneous nucleation (figure 1(c)). Then, choosing the different β, K_1 and K_2, one needs to investigate their influence on the hysteresis. The result is shown in figure 7. Hereby the set of parameters is, again, the above-mentioned one with the additional $\beta_1 = 1$, $\beta_2 = 0.75$, $\beta_3 = 0.5$, $\beta_4 = 0.25$ and $\beta_5 = 0$.

We see that the shape of hysteresis essentially depends on the value β (two-petal-shaped hysteresis for $0 < \beta < 1$). The changing of β leads to crossover from petal-shaped hysteresis at $\beta = 1$ with one width to another petal-shaped hysteresis at $\beta = 0$ with a different width (via double-petal-shaped hysteresis).

5. Summary and concluding remarks

The kinetics of nucleation–growth and separation processes in a nanopowder under the external temperature field is presented. The model has allowed us to make several distinct conclusions, clarifying the specific feature of phase separation phenomenon in nanovolumes.

Based on our numerical studies, we conclude that for the fixed conditions of temperature cycling one should observe hysteresis behaviour. Such hysteresis is conditioned by the finite size and depletion effects and is shown on the basis of the kinetic equation approach.

The model shows that the width of the hysteresis loop depends on

(i) thermodynamic constraints (N_0, K, δ, β) at the fixed rate of temperature changes ($\mathrm{d}T/\mathrm{d}\tau$) and other parameters;
(ii) kinetic constraints (Q).

In particular, as

(a) the size of a system,
(b) the rate of temperature changes,
(c) the interphase tension,
(d) the energy barrier for diffusion,

decrease, the hysteresis loop narrows, showing a tendency to disappearance.

Besides this, the shape of hysteresis appreciably depends on the nucleation mechanisms (β). This becomes apparent particularly in the case of large scatter of particle sizes [19]. In the case of lognormal distribution the scatter in particle sizes leads to increase of the hysteresis width.

The given approach allows us to distinguish the influence of thermodynamic constraints on hysteresis (related to the Gibbs free energy dependence on size and nucleation barrier) from the influence of kinetic constraints on hysteresis (related to the activation energy for the diffusion across the parent phase–nucleus interface). At high T the hysteresis is related to a thermodynamic controlled process, whereas at low T the hysteresis is related to a kinetic controlled process.

In the present model we have used simplifications, some of which have been discussed above. For example, the structural transitions without diffusion redistribution (polymorphic transitions) have been neglected. Such transitions between different crystal modifications can be important for first order phase transitions in nanovolumes [16, 17]. The corresponding analysis will be presented elsewhere.

Also, so-called bulk metallic glasses [27, 28] often devitrify with a very high nucleation rate yielding, in a first crystallization stage, a dispersion of nanocrystals in the amorphous matrix [29]. This means that precipitation develops in nanometric volumes, which can be realized in nanometric spherical regions (of radius R) around nucleation sites. One should expect the similar hysteresis behaviour in bulk metallic glasses due to the depletion and the size effects shown in present paper. We suppose that in the case of multidefect alloy on equidistant heterogeneous nucleation sites one should expect the possibility of spontaneous transition in the temperature region confined within the up and down values (depending on the size of the nucleation–growth region). The corresponding analysis will be made elsewhere.

Another intriguing extension should involve the cases of (i) competitive formation in the nanoparticle of two and/or more phases with different stoichiometries and (ii) multicomponent systems. The model introduced may also be useful in the analysis of other phase transitions in small systems (nanoporous materials) and is closely related to present-day problems. For example, as follows from our results, one can use the size-induced hysteresis behaviour for computer disk recording where the phase transition mentioned here (nonmagnetic) occurs during the temperature cycling.

Acknowledgments

This work has been carried out within the frame of the International Association for Promotion of Cooperation with Scientists from New Independent States of the former Soviet Union (Young NIS Scientist Fellowships Programme 2003, Intas reference No 03-55-1169). The work was also partially supported by the Ministry of Education and Science of Ukraine. MOP thanks the US Civilian Research and Development Foundation (award No UE1-2523-CK-03).

Appendix. Effect of scatter in particle sizes

Here we present an analysis of the thermodynamics and kinetics of transition phenomena in a nanopowder, taking into account the possible size distribution of the nanoparticles. From this, it is seen that the effect of distribution on particle sizes may change the picture of collective formation of the new phase. Consequently, the change of Gibbs potential (4), instead of a function of a nucleus size, becomes then a functional of the distribution of sizes N_0.

Let us introduce the value $\bar{N}_0$ as the most probable size of the nanoparticles (nearly equal mean sizes) of the nanopowder and δ as the standard deviation ($\delta < 1$) of size distribution function $\phi(N_0|\delta)$ (here, the number of particles consisting of N_0 atoms). In the case of equal size particles $\bar{N}_0 = N_0$. In the following, we treat the different values of δ as the criterion of the different scatter in sizes of particles.

We have formulated our analysis for the distribution function $\phi(N_0|\delta)$ with the different δ of size distribution in the analytical coherent scheme (A.1) as well as in the discrete approach (A.2). Further, we present the second mode as approximate to the numerical analysis developed above as well as to experimental analysis [18, 19, 26].

Continuous Gaussian and lognormal distributions, respectively,

$$\begin{aligned}\phi_1(N_0|\delta) &= \frac{W}{\sqrt{2\pi}\,\delta\bar{N}_0}\exp\left\{-\frac{(N_0-\bar{N}_0)^2}{2\delta^2\bar{N}_0^2}\right\},\\ \phi_2(N_0|\delta) &= \frac{W}{\sqrt{2\pi}\,\delta N_0}\exp\left\{-\frac{[\ln(N_0)-\ln(\bar{N}_0)-\delta^2]^2}{2\delta^2}\right\}.\end{aligned} \tag{A.1}$$

For the second discrete mode we divided the total number of particles W into ten groups W_i of different sizes N_{0i} ($i = \overline{1,10}$) each. Such a procedure is quite sufficient to describe the small deviations δ. Discrete distributions (and groups) are expressed by using the mass conservation:

$$W = \sum_{i=1}^{10} W_i, \qquad N_0 W = \sum_{i=1}^{10} N_{0i} W_i. \tag{A.2}$$

For example, a Gaussian distribution with $\delta = 0.2$ and $\bar{N}_0 = 1000$ is presented in table A.1.

In a similar manner, the discrete lognormal distribution is given in table A.2.

Thus, the different values N_{0i} and the corresponding groups W_i form the discrete distributions (A.2). For further illustration, we present figure A.1 (see also qualitative figures 1(b) and (c)).

Under the chosen conditions, the change of Gibbs free energy $\Delta G(N,T)$ becomes a function of sizes N_{0i} as well:

$$\begin{aligned}\Delta G(N,N_{0i},T) &= \Delta g_1(T)\frac{N}{C_1} + \Delta g_0(T,C_\mathrm{p})\\ &\times\left\{N_{0i}-\frac{N}{C_1}\right\} - \Delta g_0(T,C_0)N_{0i} + K\left\{\frac{N}{C_1}\right\}^{\frac{2}{3}}.\end{aligned} \tag{A.3}$$

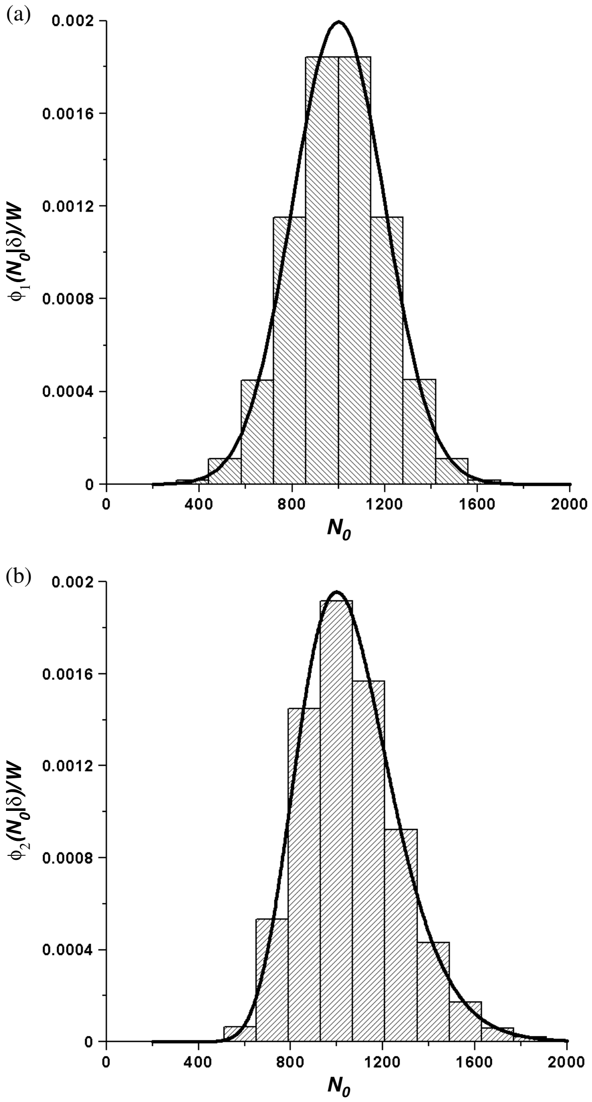

Figure A.1. The almost symmetric Gaussian distribution (a) and the asymmetric lognormal distribution (b) of particles in a nanopowder (standard deviation $\delta = 0.2$).

The conservation law (3) must be modified as $C_0 N_{0i} = C_1 N_1 + C_\mathrm{p} N_\mathrm{p}$.

Furthermore, similar reasoning is applied to the equilibrium distribution function of the given i-group:

$$\begin{aligned}f_{\mathrm{eq},i}(N,N_{0i},T) &= \frac{W_i}{\sum_{N=N_\mathrm{min}}^{N_\mathrm{max}(i)}\exp\{-\frac{\Delta G(N,N_{0i},T)}{kT}\}}\\ &\times\exp\left\{-\frac{\Delta G(N,N_{0i},T)}{kT}\right\}.\end{aligned} \tag{A.4}$$

Hereby the upper limit of the sum in (A.4) is given by $N_\mathrm{max}(i) = C_0 N_{0i}/C_1$.

The average equilibrium distribution function is determined by the formula

$$\bar{f}_\mathrm{eq}(N,T) = \frac{\sum_{i=1}^{10} f_{\mathrm{eq},i}(N,N_{0i},T)}{W}.$$

Table A.1. Discrete distribution coinciding with the Gaussian distribution (A.1), where $\delta = 0.2$ and $\bar{N}_0 = 1000$.

i	1	2	3	4	5	6	7	8	9	10
W_i/W	0.002 32	0.015 30	0.062 88	0.161 22	0.258 12	0.258 18	0.161 33	0.062 95	0.015 32	0.002 32
N_{0i}	393	528	663	798	932	1067	1201	1336	1471	1606

Table A.2. Discrete distribution coinciding with the lognormal distribution (A.1) with $\delta = 0.2$ and $\bar{N}_0 = 1000$.

i	1	2	3	4	5	6	7	8	9	10
W_i/W	0.009 10	0.074 76	0.202 98	0.268 59	0.219 65	0.129 20	0.060 40	0.024 00	0.008 50	0.002 77
N_{0i}	611	737	866	999	1135	1272	1410	1548	1687	1826

Combining (A.2)–(A.4) and the definition (6), we obtain corresponding mean equilibrium values:

$$\begin{aligned}\langle C_{\mathrm{p}}^{\mathrm{eq}}\rangle &= \left\{\sum_{i=1}^{10}\sum_{N=N_{\min}}^{N_{\max}(i)} C_{\mathrm{p}}(N,N_{0i})\, f_{\mathrm{eq},i}(N,N_{0i},T)\right.\\ &\quad\times\left.\left\{N_{0i}-\frac{N}{C_1}\right\}\right\}\left\{\sum_{i=1}^{10}\sum_{N=N_{\min}}^{N_{\max}(i)} f_{\mathrm{eq},i}(N,N_{0i},T)\right.\\ &\quad\times\left.\left\{N_{0i}-\frac{N}{C_1}\right\}\right\}^{-1},\\ \langle\rho_{\mathrm{eq}}\rangle &= \frac{\sum_{i=1}^{10}\sum_{N=N_{\min}}^{N_{\max}(i)}\frac{N}{C_1} f_{\mathrm{eq},i}(N,N_{0i},T)}{\sum_{i=1}^{10} N_{0i}W_i}.\end{aligned}\qquad (A.5)$$

Now it is easy to find the nonequilibrium distribution function $f_i(N,\tau)$ for each group i, at any fixed N_{0i}. The corresponding kinetic equation for $f_i(N,\tau)$ has a form similar to equation (7). Hereby one needs to introduce the $f_i(N,\tau)$ instead of $f(N,\tau)$ in equation (7). Also, the quantities $v_+(N,\tau)$, $v_-(N,\tau)$ and $\Delta G(N,T)$ must be replaced by the corresponding values $v_+(N,N_{0i},\tau)$, $v_-(N,N_{0i},\tau)$ and $\Delta G(N,N_{0i},T)$, respectively, in equation (8). The boundary conditions (9) can be found as

$$\begin{aligned} f_i(N_{\min},\tau) &= W_i - \sum_{N=N_{\min}+1}^{N_{\max}(i)} f_i(N,\tau),\\ f_i(N_{\max}(i),\tau) &= 0,\\ f_i(N,\tau=0) &= \begin{cases} W_i, & N = N_{\min}\\ 0, & N \neq N_{\min}.\end{cases}\end{aligned}\qquad (A.6)$$

As mentioned above, our aim is to determine the values of $\langle C_{\mathrm{p}}\rangle$ and ρ:

$$\begin{aligned}\langle C_{\mathrm{p}}\rangle &= \frac{\sum_{i=1}^{10}\sum_{N=N_{\min}}^{N_{\max}(i)} C_{\mathrm{p}}(N,N_{0i}) f_i(N,\tau)\{N_{0i}-\frac{N}{C_1}\}}{\sum_{i=1}^{10}\sum_{N=N_{\min}}^{N_{\max}(i)} f_i(N,\tau)\{N_{0i}-\frac{N}{C_1}\}},\\ \langle\rho\rangle &= \frac{\sum_{i=1}^{10}\sum_{N=N_{\min}}^{N_{\max}(i)}\frac{N}{C_1} f_i(N,\tau)}{N_0 W}.\end{aligned}\qquad (A.7)$$

The corresponding analysis of the influence of different distributions and deviations δ is presented in section 4.6.

References

[1] Couchman P R and Jesser W A 1977 *Nature* **269** 481
[2] Nagaev E L 1992 *Usp. Fiz. Nauk* **162** 50
[3] Pawlow P 1909 *Z. Phys. Chem.* **65** 1
[4] Buffat Ph and Borel J P 1976 *Phys. Rev.* A **13** 2287
[5] Wautelet M 2000 *Nanotechnology* **11** 6
[6] Rossi G, Rapallo A, Mottet C, Fortunelli A, Baletto F and Ferrando R 2004 *Phys. Rev. Lett.* **93** 105503
[7] Petrov Y I 1982 *Physics of Small Particles* (Moscow: Science)
[8] Gladgkikh M T, Chigik S P, Larin V N, Grigorijeva L K and Suhov V N 1988 *Dokl. Akad. Nauk USSR* **300** 588
[9] Rusanov A I 1967 *Phase Equilibriums and Surface Phenomena* (Leningrad: Chemistry)
[10] Ulbricht H, Schmelzer J, Mahnke R and Schweitzer F 1988 *Thermodynamics of Finite Systems and Kinetics of First-Order Phase Transitions* (Leipzig: Teubner)
[11] Gusak A M and Shirinyan A S 1998 *Met. Phys. Adv. Tech.* **20** 40
[12] Ludwig F P and Schmelzer J 1996 *J. Colloid Interface Sci.* **181** 503
[13] Shirinyan A S and Gusak A M 2004 *Phil. Mag.* A **84** 579
[14] Jesser W A, Shneck R Z and Gille W W 2004 *Phys. Rev.* B **69** 144121
[15] Pochon S, MacDonald K F, Knize R J and Zheludev N I 2004 *Phys. Rev. Lett.* **92** 145702
[16] Jacobs K, Zaziski D, Scher E C, Herhold A B and Alivisatos A P 2001 *Science* **293** 1803
[17] Chen C C, Herhold A B, Johnson C S and Alivisatos A P 1997 *Science* **276** 398
[18] Kamenev K, Balakrishnan G, Lees M R and Paul DMcK 1997 *Phys. Rev.* B **56** 2285
[19] Qadri S B, Skelton E F, Hsu D, Dinsmore A D, Yang J, Gray H F and Ratna B R 1999 *Phys. Rev.* B **60** 9191
[20] Neimark A, Ravikovitch P I and Vishnyakov A 2002 *Phys. Rev.* E **65** 1505
[21] Shirinyan A S, Gusak A M and Desre P J 2000 *J. Metast. Nanocryst. Mater.* **7** 17
[22] Shirinyan A S and Wautelet M 2004 *Nanotechnology* **15** 1720
[23] Schmelzer J and Schweitzer F 1990 *Z. Phys. Chem.* **271** 565
[24] Bartels J and Schmelzer J 1992 *Phys. Status Solidi* a **132** 361
[25] Baletto F, Mottet C and Ferrando R 2003 *Phys. Rev. Lett.* **90** 135504
[26] Carpenter D T, Codner J R, Barmak K and Rickman J M 1999 *Mater. Lett.* **41** 296
[27] Inoue A, Zhang T and Masumoto T 1990 *Mater. Trans. JIM* **31** 425
[28] Paker A and Johnson W L 1993 *Appl. Phys. Lett.* **63** 2342
[29] Calin M and Koster U 1997 *Mater. Sci. Forum* **269–272** 749